Available online at www.sciencedirect.com
SCIENCE DIRECT®
Biochemical and Biophysical Research Communications 337 (2005) 127–132
BBRC
www.elsevier.com/locate/ybbrc

Phototoxicity of Hemoporfin to ovarian cancer

Kun Song [a], Beihua Kong [a,*], Xun Qu [b], Li Li [a], Qifeng Yang [c,d]

[a] Department of Obstetrics and Gynecology, Qilu Hospital, Shandong University, Ji'nan 250012, Shandong, PR China
[b] Department of Basic Medicine, Qilu Hosptial, Shandong University, Ji'nan 250012, Shandong, PR China
[c] The Cancer Institute of New Jersey, Robert Wood Johnson Medical School, New Brunswick, NJ 08903, USA
[d] Department of Genetics, Rutgers, The State University of New Jersey, Piscataway, NJ 08854, USA

Received 1 September 2005
Available online 15 September 2005

Abstract

Hematoporphyrin monomethyl ether (Hemoporfin) is a novel porphyrin-related photosensitizer. Photocytotoxic effect of Hemoporfin to ovarian cancer is still unclear. We used human epithelial ovarian carcinoma cell line SKOV3 and its xenograft model in nude mice to investigate the Hemoporfin-based photodynamic therapy (PDT) for ovarian cancer. The growth rates of SKOV3 cells were determined by MTT assays. Flow cytometry combined with dual Annexin V/PI staining was used to identify the death mode of the cells following PDT. We demonstrated that Hemoprofin-based PDT induced significant cell death via direct necrosis induction, and the photocytotoxity to SKOV3 cells is dose related. With SKOV3 xenograft model in nude mouse, we further demonstrated that Hemoporfin-based PDT is effective for controlling the tumor growth. Our results suggest that Hemoporfin is a promising novel photosensitizer for the treatment of ovarian cancer and merit further evaluation in the clinical practice.

Keywords: Ovarian cancer; Hematoporphyrin monomethyl ether; Photodynamic therapy

Ovarian cancer is the sixth most common cancer and cause of death from cancer in women in the world, with approximately 165,000 new cases and 101,000 deaths anticipated every year [1]. Due to the lack of effective prevention and screening modalities, the majority of patients who are diagnosed with epithelial ovarian cancer present with advanced-staged disease [2]. During the past decade, advances in surgical technique and chemotherapy have resulted in response rates that exceed 70%; however, most patients with advanced-stage ovarian cancer recur and ultimately died of their disease [3]. These ominous statistics justify the search for effective new therapies, such as photodynamic therapy, for patients afflicted with ovarian cancer.

Photodynamic therapy (PDT) is a promising new cancer treatment strategy that involves the combination of visible light and a photosensitizer [4,5]. Each factor is harmless by itself, but when combined with oxygen, they can produce lethal cytotoxic agents that can inactivate tumor cells. This enables greater selectivity towards diseased tissue as only those cells that are simultaneously exposed to the photosensitizer, light, and oxygen are exposed to the cytotoxic effect. The dual selectivity of PDT is produced by both a preferential uptake of the photosensitizer by the diseased tissue and the ability to confine activation of the photosensitizer to this diseased tissue by restricting the illumination to that specific region. Therefore, PDT allows for the selective destruction of tumors while leaving normal tissue intact.

The first generation of photosensitizers are hematoporphyrin derivatives (HpD), such as Photofrin which is still the most commonly used photosensitizer in clinical PDT but has the drawbacks such as a long-term skin photosensitization and a poorly defined chemical composition which makes a detailed understanding of its mode of action and pharmacokinetics difficult. To overcome its drawbacks, the second generation of photosensitizers are being developed and a number of new agents are now in clinical trials [6,7]. Hematoporphyrin monomethyl ether (HMME, Hemoporfin) is a novel porphyrin-related photosensitizer

* Corresponding author. Fax: +86 531 82949225.
E-mail address: kongbeihua@sdu.edu.cn (B. Kong).

0006-291X/$ - see front matter © 2005 Elsevier Inc. All rights reserved.
doi:10.1016/j.bbrc.2005.09.021

that was developed first in China. Hemoporfin consists of two monomer porphyrins, namely, 3-(1-methyloxyethyl)-8-(1-hydroxyethyl)deuteroporphyrin IX and 8-(1-methyloxyethyl)-3-(1-hydroxyethyl)deuteroporphyrin IX, that are mutually locational isomers. Experimental studies and clinical trials have shown that Hemoporfin has a higher selective uptake by tumor tissue, stronger photodynamic effect, lower toxicity, and shorter-term skin phototoxicity than HpD, and is a promising photosensitizer for tumor PDT [8]. In this study, we are interested to characterize the basic features of this new photosensitizing drug. Furthermore, we will investigate the photocytotoxic effect of Hemoporfin on ovarian cancer.

Materials and methods

Cell line and animals. Human epithelial ovarian cancer cell line SKOV3 was obtained from Basic Medicine Research Institute, Qilu hospital, Shandong University, PR China. Cells were cultured in RPMI-1640 medium (Gibco Life Technologies) enriched with 10% heat-inactivated fetal calf serum (FCS; Gibco) and incubated under standardized conditions (37 °C, 5% carbon dioxide, 100% humidity). Pathogen-free female Balb/c nude mice (WeiTongLiHua, Beijing, China), weighing 18–20 g, were housed in a pathogen-free animal facility and given commercial basal diet.

Hemoporfin and absorption spectrum determination. Hemoporfin hydrosolvent was provided by the Shanghai FuDan-ZhangJiang Bio-Pharmaceutical (Shanghai, China). Hemoporfin solution was prepared freshly prior to use by dissolving in phosphate-buffered saline (PBS) at a concentration of 10 mg/ml and kept in dark at 4 °C. Further dilution of Hemoporfin was performed in serum-free RPMI 1640 medium to reach different concentrations.

Visible absorption spectra of Hemoporfin in different solvents were investigated. Hemoporfin was diluted to 0.4 mg/ml in FCS-free RPMI 1640 medium, 10% FCS RPMI 1640 medium, and full FCS, respectively. Absorption spectra were scanned in 400–800 nm with the SHIMADZU UV-2401 spectrophotometer (SHIMADZU Instruments, Japan).

Intracellular Hemoporfin observation. To investigate the kinetics of intracellular distribution of Hemoporfin, 1×10^4 SKOV3 cells were seeded per well in 12-well plates and allowed to adhere and acclimate for 2 days. Then, 500 μl of medium containing Hemoporfin (30 μg/ml) was applied to cells and incubated for different intervals at 37 °C with light protection. After three phosphate-buffered saline (PBS) washes, fluorescent images were acquired with an OLYMPUS IX81 inverted fluorescence biomicroscope equipped with a DP30BW intensified charge-coupled device (ICCD). Three excitation and emission filters with wavelengths at 330–380, 450–480, and 510–550 nm were used, images were captured using a UPLSAPO objective and ICCD camera, and subsequently processed using Image-Pro software (MediaCybernetics, USA). JD801 Image analysis system (JieDa, JiangSu, China) was applied to measure the fluorescence intensity of Hemoporfin in the cells.

To further determine the intracellular localization of Hemoporfin in SKOV3 cells, a sterile quartz coverslip (0.5 mm diameter, 0.2 mm thick) was placed onto the bottom of 35 mm petri dishes, 1×10^5 cells were seeded and cultured for 2 days. For Hemoporfin treatment, the medium was aspirated and replaced with medium containing Hemoporfin (40 μg/ml). Following 3 h incubation, the cells were rinsed three times with PBS and examined immediately with an OLYMPUS FLUOVIEW 500 scanning laser confocal microscope (OLYMPUS, Japan). Two types of excitation waves (515 and 543 nm) were generated by multi-line argon ion laser and the helium–neon laser, respectively. The emission wavelengths were larger than 610 nm. Fluoview (version 4.3) was used to encode and process the fluorescence images.

In vitro photodynamic therapy. SKOV3 cells in 200 μl of 10% FCS RPMI 1640 medium (1.5×10^4 cells/well) were incubated in the 96-well flat-bottomed microtiter plates at 37 °C in a 5% CO_2 incubator. When cells were in exponential growth phase, the supernatants were removed and replaced with 200 μl fresh FCS-free medium. The cells were incubated with varying concentrations of Hemoporfin (0–50 μg/ml) for 3 h. The medium containing the drug was then aspirated and the cells were rinsed with PBS and then replacing with another 200 μl RPMI 1640 before illumination. The laser source was a pulsed dye laser (Quantel Datachrom 5000, Quantel, French) operating at a frequency of 10 Hz. Irradiation was carried out at different light doses (0–12 J/cm^2) at 620 nm with an output of 160 mW. Following this treatment, medium was replaced by 10% FCS RPMI 1640 and the cells were grown on again for a further 24 h. To evaluate cell viability and thus calculate the percentage of phototoxicity, 3-(4,5-dimethylthiazol-2-yl)-2,5-diphenyltetrazolium bromide (MTT) assay was employed.

Phototoxicity assay. The MTT assay was used to determine photosensitizer-mediated cytotoxicity, as described previously [9,10]. Briefly, target tumor cells were resuspended in medium at 1×10^5 cells/ml after verifying cell viability by trypan blue dye (Sigma Chemical) exclusion assay. One hundred microliters of cell suspension was distributed into each well of a 96-well flat-bottomed microtiter plate, and each plate was incubated for 24 h at 37 °C and 5% CO_2 atmosphere. After the incubations, 100-μl reagent solutions or media at the desired concentrations were distributed into each well. The well containing only media served as a positive control. Two hundred microliters of the medium alone without cells and reagent was used as a negative control. The microtiter plate was incubated for the desired period of time. Thereafter, 20 μl of the MTT dye (5 mg/ml) was added into each well. The unreactive supernatants in the well were carefully aspirated and replaced with 100 μl of isopropanol supplemented with 0.05 N HCl to solubilize the reactive dye. The absorbance (A) values of each well at 540 nm were read using an automatic multiwell spetrophotometer (Bio-Rad-Coda, Richmond, CA). The negative control well was used for zeroing absorbance. The percentage of cytotoxicity was calculated using the background-corrected absorbance as follows:

$$\text{inhibition rate} = (1 - [A \text{ of experimental well}/A \text{ of positive control well}]) \times 100\%.$$

Experiments were performed at least three times with representative data presented.

Determination of cell death. Apoptosis or necrosis was determined by flow cytometer using the Annexin V-FITC apoptosis kit (BioVision, USA) according to the manufacturer's instructions. Briefly, about 1×10^4 cells were suspended in 100 μl Annexin V binding buffer and incubated with 10 μl Annexin V (20 μg/ml) for 15 min at room temperature in the dark. Consequently, 400 μl binding buffer containing 5 μl propidium iodide (PI, 50 μg/ml) was added and incubated on ice for additional 15 min. Then the cells were analyzed with a FacsCalibur flow cytometer (Becton–Dickinison, USA) within 1 h. Data analysis was performed with CELLQuest software (Becton–Dickinison, USA). Experiments were performed at least three times with representative data presented. The results were interpreted as follows: cells that were Annexin V(−)/PI(−) (lower left quadrant) were considered as living cells, the Annexin V(+)/PI(−) cells (lower right quadrant) as apoptotic cells, Annexin V(+)/PI(+) (upper right quadrant) as necrotic or advanced apoptotic cells, and Annexin V(−)/PI(+) (upper left quadrant) may be bare nuclei, cells in late necrosis, or cellular debris.

Apoptosis was further measured by evaluating the sub-G1 cell population with single PI staining. Briefly, cells were fixed by 75% ice-cold ethanol with vigorous shaking and kept at 4 °C overnight. After centrifugation, cells were collected and incubated with 200 μl RNase A (1 mg/ml) at 37°C for 30 min and then stained by using 800 μl (100 μg/ml) PI at 37 °C for 30 min. Apoptosis analysis was performed in a FACScan (FL-2 channel, Becton–Dickinson, San Jose, CA, USA) based on propidium iodide staining, cells in the sub-G1 marker window were considered to be apoptotic.

In vivo phototoxicity assay. The SKOV3 cells were harvested with 0.25% trypsin (Gibco) from tissue culture flasks and washed twice with 0.9% NaCl solution. A total of 1×10^7 cells were subcutaneously (s.c.) injected into the right flank of Balb/c nude mice. Twenty tumor-bearing

mice were divided into four groups. One of them is PDT group ($n = 5$): mice were injected i.p. (intraperitoneal) with Hemoporfin (10 mg/kg). The dose of Hemoporfin is based on the provider's pharmacokinetic and toxic experiments (data not shown). One hour after injection, mice were illuminated with light (620 nm). A pulsed dye laser (Datachrom 5000, Quantel, French) was used to deliver light bundle. A power density of 100 mW/cm^2 was chosen to deliver light dose 120 J/cm^2 to the tumor site. The laser power was measured with a Power Meter (Newport, Irvine, CA). After treatment, the mice were housed free of light for 3 days. The other three groups were controls: (1) mice received 0.9% NaCl injection i.p. ($n = 5$); (2) mice received 0.9% NaCl injection i.p. following by light exposure ($n = 5$); (3) mice received Hemoporfin injection without light exposure ($n = 5$). Tumor volume was assessed by measuring two axes (R_1, R_2) and calculated using the formula: $V = 1/6\pi R_1^2 R_2$. To assess the response to treatment, two indexes, *D4* and *D8*, were defined:

D4 = (tumor volume at day 4 after PDT)/(tumor volume before PDT),

D8 = (tumor volume at day 8 after PDT)/(tumor volume before PDT).

Tumor regression rate (TRR) was also calculated by using the following formula:

$$\mathrm{TRR}(\%) = [1 - (V_{\text{after-before}}/V'_{\text{after-before}})] \times 100\%,$$

where V means the tumor volume in PDT group and V' in controls.

Statistical analysis. The statistical analysis was performed using SPSS 11.5 for Windows. Differences between groups were analyzed by Student's t test. A value of $p < 0.05$ was regarded as being statistically significant.

Results

Absorption spectrum of Hemoporfin

Three types of solvents were irradiated with UV-A, no signals were observed. However, when Hemoporfin was dissolved in the solvents, signals were observed in the solution containing Hemoporfin with UV-A irradiation. The results indicated that the signals were derived from Hemoporfin. Hemoporfin exhibited four absorption bands in the wavelength range from 400 to 800 nm, and similar peaks were shown in solutions with different kinds of solvents (Fig. 1). The peak on 620 nm could be chosen as light source for PDT.

Intracellular distribution of Hemoporfin

The intracellular distribution of Hemoporfin in the SKOV3 was examined using fluorescence microscopy and confocal microscopy. Untreated SKOV3 cells showed no fluorescence. After 30 μg/ml of Hemoporfin incubation, red fluorescence in the cells was identified. It is more distinct in confocal microscopy images than in fluorescence microscopy images that the dye appeared to be distributed widely throughout the cytoplasm in a punctate pattern (Fig. 2). Fluorescence density analysis showed that optical density reached a peak after incubation of 3 h in SKOV3 cells, which indicated that the optimal photodynamic treatment time is 3 h after photosensitizer administration.

In vitro phototoxicity

MTT assay showed that phototoxicity was related with Hemoporfin concentration but less affected by light dose in a given concentration (Fig. 3). If no light was exposed to the cells, lower concentration (<30 μg/ml) of Hemoporfin did not influence cell survival. However, higher concentration (>40 μg/ml) of Hemoporfin decreased the cell survival, which indicated its dark toxicity. A maximum level of phototoxicity was achieved when the drug dose reached 30 μg/ml. The survival rate didn't decrease while the concentration increased >40 μg/ml.

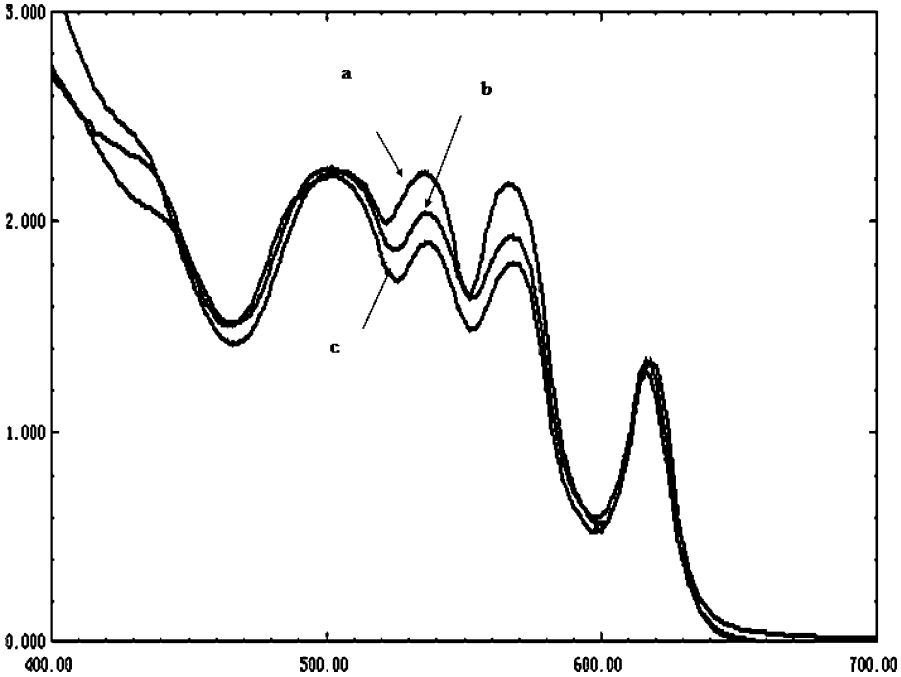

Fig. 1. UV–VIS absorption spectra of Hemoprofin in three types of media; (a) FCS-free RPMI 1640; (b) 10% FCS RPMI 1640; (c) Full FCS. FCS means heat-inactivated fetal calf serum.

Fig. 2. Laser confocal scanning microscopy (LCSM) observation of SKOV3 cancer cells after Hemoprofin incubation (400×). Fluorescence is observed in the cytoplasm.

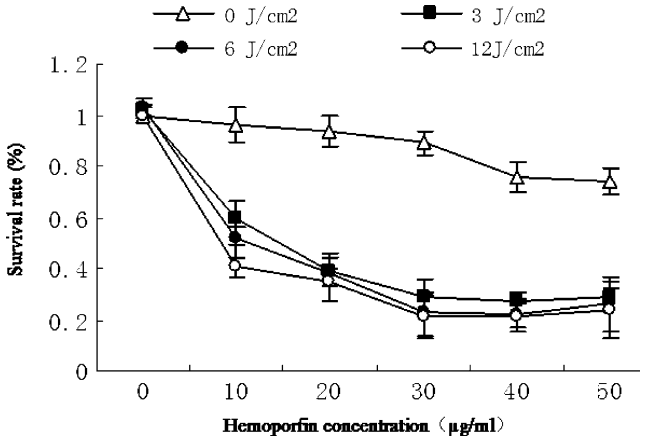

Fig. 3. Photocytotoxity of Hemoporfin to SKOV3 cancer cells. Shown are the cell survival rates at 24 h after PDT with different concentrations of Hemoporfin and different light doses.

Dual staining of cells with Annexin V and PI can distinguish early apoptotic from late apoptotic or necrotic cells. After photodynamic treatment, represented SKOV3 cell samples were subjected to cell death mechanism assay. Flow cytometry dot plots of the simultaneous binding of Annexin V-FITC and PI uptake by cells are presented in Fig. 4. The cells were characterized by Annexin V(+)/PI(+), which represented necrosis or advanced apoptosis. Single PI staining and flow cytometry of cells (Fig. 5) showed no hypodiploid peak in the treated cells, indicating that no apoptosis occurred in the SKOV3 cells with Hemoporfin-based PDT. Therefore, Hemoporfin-based PDT induced direct necrosis rather than through apoptosis in SKOV3 cells.

Effectiveness of Hemoporfin-based PDT in tumor model

SKOV3 cells were subcutaneously injected into the right flank of Balb/c nude mice. Five to seven days following injection, the primary tumor became palpable. Three weeks after implantation, tumors reached the appropriate size of around 0.5 cm^3 and Hemoporfin-based PDT was started. The time-course of tumor volume change is shown in Fig. 6. The application of Hemoporfin or light alone did not cause any measurable effects on tumor growth compared to blank group. It is noteworthy that tumor volume of PDT group dramatically reduced within 10 days after PDT. The effectiveness of the PDT to tumor-bearing mice was evaluated by calculating the tumor volume change before and after PDT. *D4* and *D8* indexes are shown in Table 1. Compared with control groups, tumor volume of PDT group shrunk significantly at both day 4 ($p < 0.05$) and day 8 ($p < 0.05$). As shown in Table 2, *TRR* exceeded 80% in the PDT group compared with controls ($p < 0.05$, respectively).

Discussion

The poor prognosis of advanced ovarian cancer and recent developments in photomedicine have generated a considerable interest in PDT for this disease. Tochner et al. [11,12] have successfully treated ovarian cancer nodules on the peritoneal surface with laser-light activated HpD in mice. Similarly, intraperitoneal benzoporphyrin derivative mono-acid ring A (BPD-MA)-mediated PDT has been used to treat epithelial ovarian carcinomatosis in a mouse model, resulting in prolongation of survival [13]. Clinical studies also showed favorable results of photodynamic therapy for cancer patients [14–16]. Hemoporfin is a novel second generation of photosensitizers, we provided the evidences that Hemoporfin is a novel photosensitizer for ovarian cancer treatment.

The photosensitizer should be excited with light of a wavelength corresponding to an absorption peak of the sensitizer. To identify possible absorption peaks, we used

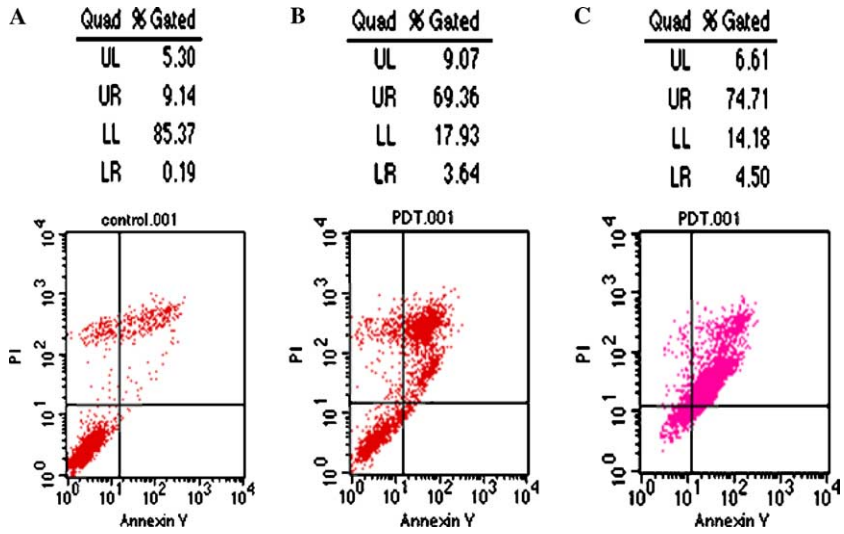

Fig. 4. Flow cytometry analysis of SKOV3 cancer cells with Annexin V/PI double staining after photodynamic therapy (PDT). (A) Controls; (B) 4 h after PDT; (C) 24 h after PDT. UL (up left quadrant), Annexin V(−) PI(+), cell fragment; UR (up right quadrant), Annexin V(+) PI(+), necrosis or the late period apoptosis; LL (low left quadrant), Annexin V(−) PI(−), survival cell; LR (low right quadrant), Annexin V(+) PI(−), early period apoptosis.

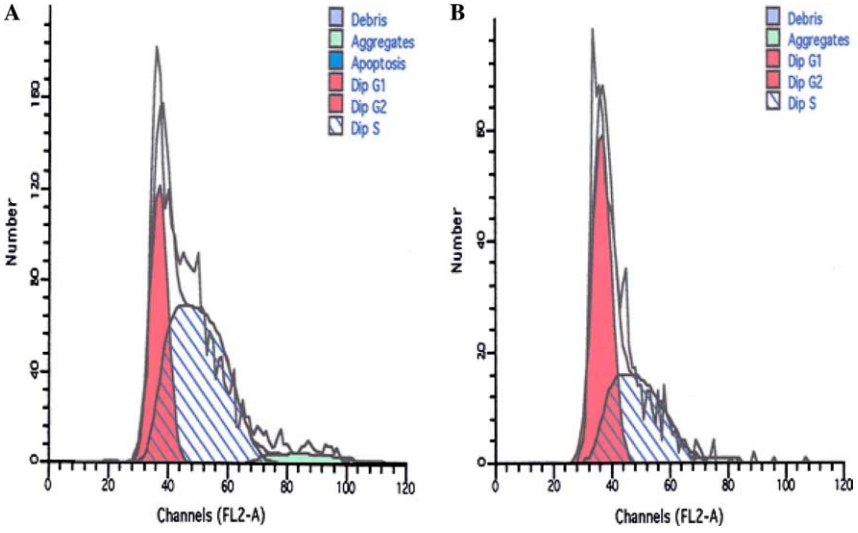

Fig. 5. Flow cytometry analysis of SKOV3 cells with single propidium iodide staining. No hypodiploid peak is identified in cancer cells at 4 h (A) or 24 h (B) after photodynamic therapy, indicating no apoptosis occurs.

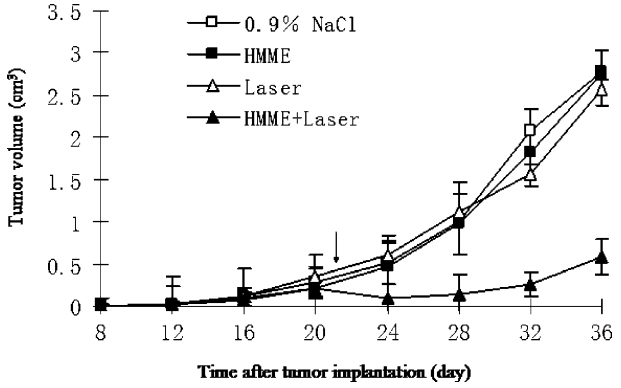

Fig. 6. Tumor volumes change after Hemoporfin-based photodynamic treatment therapy in an animal model. Hemoporfin (10 mg/kg) was injected intraperitoneally following by illumination (120 J/cm^2) to the tumor site at day 22 (indicated with arrow).

Table 1
D4 and *D8* indexes with experimental treatment in the animal model

	Control	Hemoporfin alone	Laser alone	PDT
D4	1.81 ± 0.20	2.29 ± 0.62	1.75 ± 0.20	$0.49 \pm 0.40^*$
D8	3.55 ± 1.85	4.8 ± 1.56	3.21 ± 0.59	$0.67 \pm 0.58^*$

* $p < 0.05$ when *D4* and *D8* in the PDT group compared with other groups.

higher concentration Hemoporfin for visible absorption spectra assay, and we demonstrated that Hemoporfin has four absorption peaks. An absorption peak at 620 nm is an ideally matched laser wavelength for PDT, especially for disseminated intraperitoneal tumors such as ovarian cancer. Light at 620 nm permits a limited penetration depth of normal tissue in the abdominal cavity and so severe toxicity such as bowel perforations could be avoided [15].

Table 2
Tumor regression rate (TRR) with experimental treatment in animal model

Group	n	$V_{after} - V_{before}$ (cm^3)[a]	TRR (%)	p[b]
Control	5	2.49 ± 0.30	84.6 ± 12.0	0.009
Hemoporfin	5	2.55 ± 0.89	84.9 ± 12.1	0.008
Laser	5	2.21 ± 0.10	82.6 ± 15.5	0.008
PDT	5	0.39 ± 0.33		

[a] V_{after} and V_{before} are the tumor volumes after and before treatment.
[b] TRR in PDT group compared to other three groups, respectively.

Hemoporfin is a porphyrin-related photosensitizer which is lipophilic and has a high propensity to accumulate in the membrances of intracellular organelles, e.g., endoplasmic reticulum, mitochondria, etc. [17–19]. In our current study, fluorescence images revealed that Hemoporfin distributed widely throughout the cytoplasm in a punctate pattern. Since the intracellular sensitizer localization is crucial for photodynamic effectiveness and contributes largely to the targeted photochemical reactions relevant to the cell death mode [20], further study should be performed to elucidate the detailed subcellular organelle localization using selective fluorescent probes.

Photocytotoxity of Hemoporfin has been well demonstrated in ovarian cancer by our in vitro and in vivo studies. Ding et al. [8] reported that both necrosis and apoptosis were observed in HeLa cells receiving Hemoporfin-based PDT. However, only necrosis was observed in the SKOV3 cells receiving Hemoporfin-based PDT based on our present study. PDT can induce cell death through necrosis or apoptosis, the type of cell death triggered by PDT being dependent on the photosensitizer used, illumination conditions, oxygenation status of tissue, and the type of cells involved [20–22]. Previous [8] and our present findings suggest that type of cell death induced by Hemoporfin-based PDT is cell type related. In addition, we demonstrated that photocytotoxity of Hemoporfin was dose-dependent. However, when Hemoporfin concentration reached 30 μg/ml, the maximum phototoxicity was achieved and increasing drug dose could not reduce the cells survival rate any more. These results indicated that photosensitizer uptake by tumor cell was saturated at that point. In addition, we also found that light density had no influence on the efficacy of Hemoporfin-based PDT in vitro. Lower power density permits wider light beam outputted by laser, which will be very convenient to illuminate the ovarian cancer nodules disseminated in the peritoneal cavity. Using SKOV3 xenograft model in nude mouse, we further demonstrated that Hemoporfin-PDT is effective for controlling the tumor growth.

Results from our in vitro and in vivo studies indicated that Hemoporfin is a novel promising photosensitizer for ovarian cancer treatment. Hemoporfin-based PDT may be considered as adjuvant therapy in the first-line treatment or as salvage therapy in recurrent patients. However, a lot of laboratory studies are needed before taking it into clinical practices.

Acknowledgments

This work was supported partly by grants from Science and Technology Special Foundation from the Ministry of Health of China (No. WKZ-2000-1-04) and National Natural Science Foundation of China (No. 30271361) to B.K.

References

[1] D.M. Parkin, P. Pisani, J. Ferlay, CA Cancer J. Clin. 49 (1999) 33–64.
[2] M.B. Daly, Hematol. Oncol. Clin. North Am. 6 (1992) 729–738.
[3] P.J. Hoskins, Crit. Rev. Oncol. Hematol. 20 (1995) 41–59.
[4] L. Ayaru, S.G. Bown, S.P. Pereira, Int. J. Gastrointest. Cancer 35 (2005) 1–13.
[5] M. Schaffer, B. Ertl-Wagner, P.M. Schaffer, U. Kulka, G. Jori, E. Duhmke, A. Hofstetter, Curr. Med. Chem. 12 (2005) 1209–1215.
[6] W.M. Sharman, C.M. Allen, J.E. van Lier, Drug. Discov. Today 4 (1999) 507–517.
[7] T.J. Dougherty, J. Clin Laser Med. Surg. 20 (2002) 3–7.
[8] X. Ding, Q. Xu, F. Liu, P. Zhou, Y. Gu, J. Zeng, J. An, W. Dai, X. Li, Cancer Lett. 216 (2004) 43–54.
[9] B. Kong, W. Wang, C. Liu, L. Song, D. Ma, X. Qu, J. Jiang, X. Yang, Y. Zhang, B. Wang, M.Q. Wei, Q. Yang, In Vivo 17 (2003) 153–156.
[10] Q. Yang, L. Shan, G. Yoshimura, M. Nakamura, Y. Nakamura, T. Suzuma, T. Umemura, I. Mori, T. Sakurai, K. Kakudo, Anticancer Res. 22 (2002) 2753–2756.
[11] Z. Tochner, J.B. Mitchell, F.S. Harrington, P. Smith, D.T. Russo, A. Russo, Cancer Res. 45 (1985) 2983–2987.
[12] Z. Tochner, J.B. Mitchell, P. Smith, F. Harrington, E. Glatstein, D. Russo, A. Russo, Br. J. Cancer 53 (1986) 733–736.
[13] K.L. Molpus, D. Kato, M.R. Hamblin, L. Lilge, M. Bamberg, T. Hasan, Cancer Res. 56 (1996) 1075–1082.
[14] W.F. Sindelar, T.F. DeLaney, Z. Tochner, G.F. Thomas, L.J. Dachoswki, P.D. Smith, W.S. Friauf, J.W. Cole, E. Glatstein, Arch. Surg. 126 (1991) 318–324.
[15] T.F. DeLaney, W.F. Sindelar, Z. Tochner, P.D. Smith, W.S. Friauf, G. Thomas, L. Dachowski, J.W. Cole, S.M. Steinberg, E. Glatstein, Int. J. Radiat. Oncol. Biol. Phys. 25 (1993) 445–457.
[16] F. Wierrani, D. Fiedler, W. Grin, M. Henry, E. Dienes, K. Gharehbaghi, B. Krammer, W. Grunberger, Br. J. Obstet. Gynaecol. 104 (1997) 376–378.
[17] J. Moan, K. Berg, Photochem. Photobiol. 55 (1992) 931–948.
[18] M.H. Teiten, L. Bezdetnaya, P. Morliere, R. Santus, F. Guillemin, Br. J. Cancer 88 (2003) 146–152.
[19] Y.J. Hsieh, C.C. Wu, C.J. Chang, J.S. Yu, J. Cell Physiol. 194 (2003) 363–375.
[20] N.L. Oleinick, H.H. Evans, Radiat. Res. 150 (1998) S146–S156.
[21] N. Ahmad, H. Mukhtar, Methods Enzymol. 319 (2000) 342–358.
[22] L. Wyld, M.W. Reed, N.J. Brown, Br. J. Cancer 84 (2001) 1384–1386.